Planet. Space Sci. 1974, Vol. 22, pp. 757 to 766. Pergamon Press. Printed in Northern Ireland

THE 'ROCHE-LIMIT' OF IONOSPHERIC PLASMA AND THE FORMATION OF THE PLASMAPAUSE

J. LEMAIRE
Institut d'Aéronomie Spatiale, 3, Avenue Circulaire, B-1180 Brussels, Belgium

(*Received* 10 *October* 1973)

Abstract—The plasmapause position is determined by the innermost equipotential surface which is tangent to the 'Roche-Limit' surface of the ionospheric plasma filling the magnetosphere. When the thermal particles corotate with the Earth's angular velocity, the 'Roche-Limit' equatorial distance is $L_c = 5{\cdot}78$ $[R_E]$. When the angular convection velocity is evaluated from the quiet time electric field distribution E3 of McIlwain (1972), L_c depends on the local time. Its minimum value is then $L_c = 4{\cdot}5$ near 2400 LT, and the plasmapause shape and position satisfactorily fit the observations. The diffusive equilibrium density distribution appropriated inside the plasmasphere, becomes convectively unstable beyond $L = L_c$, where the collisionless type of model satisfactorily represents the observations. In the intermediate region between the plasmapause and the last closed magnetic field line, continuous ionization fluxes are expected to flow out of the midlatitude ionosphere.

1. INTRODUCTION

The plasmapause is generally considered as the surface of a forbidden region (the plasmasphere) where low energy protons and electrons from the magnetotail convected in the sunward direction cannot penetrate under steady state conditions. To construct theoretical plasmapause models Nishida (1966), Brice (1967), Kavanagh *et al.* (1968), Vasyliunas (1970, 1972), Grebowsky (1970, 1971), Wolf (1970), Chen and Wolf (1972) have adopted some *ad hoc* or best fit geometries for the dawn–dusk convection electric field induced across the magnetosphere by the solar wind, as described by Dungey (1961) or by Axford and Hines (1961). These theories of the plasmapause formation are based on drift path determination of zero energy protons and electrons moving outside of the plasmasphere. Figure 1 shows for instance the drift path of these particles for a uniform dawn–dusk electric field of 0·16 mV/m (Kavanagh *et al.*, 1968). The solid line in Fig. 1 is the equatorial section of this forbidden region (or zero-energy Alfvén-layer) usually identified with the plasmapause. In this interpretation the plasmapause coincides also with the drift path of the last closed magnetic field line convecting around the Earth. Field lines outside this limit reach the magnetopause where they open on the geomagnetic tail. Carpenter's (1966) observations of the knee and the plasmapause positions of Chappell *et al.* (1971) are also shown in Fig. 1.

Although the plasmasphere is often considered as the forbidden region for cold plasma originating in the magnetotail, its main property, however, is to be filled with very low energy particles evaporated from the topside ionosphere. The density distribution of these thermal particles along the magnetic field lines is determined by the gravitational and rotational potentials, ψ_g and ψ_Ω. In this paper we suggest that the plasmapause is determined by the last field line along which $\psi = \psi_g + \psi_\Omega$, the total potential energy of the ions or electrons, has one single maximum in the equatorial plane. For a corotating neutral atmosphere this would correspond to the 'Roche-Limit' located at 6·6 Earth radii, where the radial component of the centrifugal force is equal to the gravitational force (Roche, 1850). For charged particles constrained to spiral along dipolar magnetic field lines, the so called 'Roche-Limit' surface of corotating ionospheric plasma is located closer to the Earth than for a corotating neutral gas.

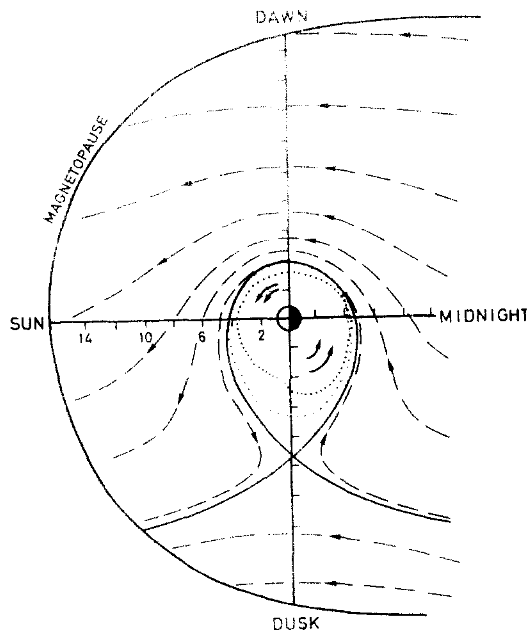

FIG. 1. ILLUSTRATION OF THE DRIFT PATH IN THE EQUATORIAL PLANE OF ZERO ENERGY PROTONS OR ELECTRONS.

The dashed lines are also electric equipotential lines in the model by Kavanagh *et al.* (1968) for a uniform dawn–dusk convection electric field of 0·16 mV/m. In this theoretical model the plasmapause is identified with the zero-energy Alfvén layer (solid line). Two different knee or plasmapause positions are shown by dots (Carpenter, 1966) and by crosses (Chappell *et al.*, 1971).

In Section 3 we describe the influence of angular rotation on the diffusive equilibrium density distribution, and deduce that it is convectively unstable beyond the 'Roche-Limit' distance.

2. THE POTENTIAL DISTRIBUTION

Let Ω be the angular drift velocity (averaged over a bounce period) for a thermal proton or electron; Ω is measured in an inertial coordinate system K: e.g. the solar-magnetospheric frame of reference. In the coordinate system K_0, rotating with angular velocity Ω, the total potential energy at the radial distance r and latitude λ is given by

$$\psi(r, \lambda) = -\frac{m_{H^+} + m_{e^-}}{2}\left[\frac{GM}{r} + \tfrac{1}{2}\Omega^2 r^2 \cos^2 \lambda\right] + c^{te} \tag{1}$$

where G is the gravitational constant, and M the mass of the Earth (see, Angerami and Thomas, 1964; Melrose, 1967). The factor $(m_{H^+} + m_{e^-})/2$ in the r.h.s. of Equation (1) results from the Pannekoek–Rosseland's charge separation electric field necessary to maintain local quasi-neutrality in a hydrogen plasma, when the electron and H^+ ion temperatures are equal (Mange, 1960).

For a dipole magnetic field, the equation of a line of force is given by

$$r = LR_E \cos^2 \lambda \tag{2}$$

where R_E is the Earth radius, and L is McIlwain's parameter characterising the equatorial distance of the line of force.

Replacing r by (2) in Equation (1), it can be shown that the total potential energy

$$\psi(\lambda; L) = -\frac{m_{\mathrm{H}^+} + m_{e^-}}{2} \frac{GM}{LR_E}\left[\frac{1}{\cos^2\lambda} + \frac{\Omega^2 R_E{}^3 L^3}{2GM}\cos^6\lambda\right] + c^{te} \tag{3}$$

has a maximum at the Equator if $L < L_c$; L_c is a critical L parameter given by

$$L_c = \left(\frac{2GM}{3\Omega^2 R_E{}^3}\right)^{1/3}. \tag{4}$$

For field lines corresponding to $L > L_c$, the potential energy has two maxima at the latitudes $\pm\lambda_m$, where

$$\lambda_m = \arccos\left(\frac{L_c}{L}\right)^{3/8}. \tag{5}$$

The corresponding radial distance is determined by

$$r_m = LR_E\left(\frac{L_c}{L}\right)^{3/4}. \tag{6}$$

Figure 2 shows the potential distribution $\psi(\lambda; L)$ in a coordinate system K_0 corotating with the Earth, along different field lines with L smaller, equal and larger than L_c.

If the ionospheric particles corotate with the Earth, (i.e. $\Omega = \Omega_E = 7{\cdot}29 \times 10^{-5}$ rad sec^{-1}) the critical L value for which the potential energy along a given field line changes from a singly peaked to a doubly peaked function is $L_c = 5{\cdot}78$. This value coincides approximately with the observed average plasmapause position at magnetically quiet time ($K_p = 0$), as reported by Binsack (1967), by Rycroft and Thomas (1970: $L_{pp} = 5{\cdot}64 - (0{\cdot}78 \pm 0{\cdot}12)\sqrt{K_p}$) or by Carpenter and Park (1973: $L_{pp} = 5{\cdot}7 - 0{\cdot}47\,K_p$).

If for any reason the mean angular drift velocity, $\Omega(\mathbf{r})$, is smaller (or larger) than Ω_E, the critical magnetic field line will cross the equatorial plane at a distance larger (or smaller) than $5{\cdot}78\ R_E$. A uniform dawn–dusk electric field can, for instance, decrease the value of Ω at dusk and consequently increase the value of L_c. The opposite occurs in the dawn sector where the convection $\mathbf{E}_{cv} \times \mathbf{B}$ drift increases the angular drift speed of the cold plasma and consequently decreases L_c. Therefore, the effect of such a steady and uniform dawn–dusk field will be to change the circular equatorial section of the 'Roche-Limit' surface into a dissymmetrical curve shifted towards the dusk sector. But the convection electric field, $\mathbf{E}_{cv}$, induced into the magnetosphere by the solar wind is not necessarily uniform nor in the dawn–dusk direction. The dashed curves in Fig. 3 represent the equipotential lines corresponding to the electric field distribution, E3, deduced by McIlwain (1972) from the observed fluxes of energetic particles encountered by the ATS 5 satellite at $6{\cdot}6\ R_E$, during low magnetic activity periods (i.e. $K_p \simeq 1$). This E3 electric field ($\mathbf{E}_{\mathrm{tot}}$) and the M2 magnetic field ($\mathbf{B}$) distributions of McIlwain (1972) can be used to calculate the actual angular drift velocity of zero-energy particles inside the whole magnetosphere.

$$\Omega(\mathbf{r}) = \frac{|(\mathbf{E}_{\mathrm{tot}} \times \mathbf{B}) \times \mathbf{r}|}{r^2 B^2}. \tag{7}$$

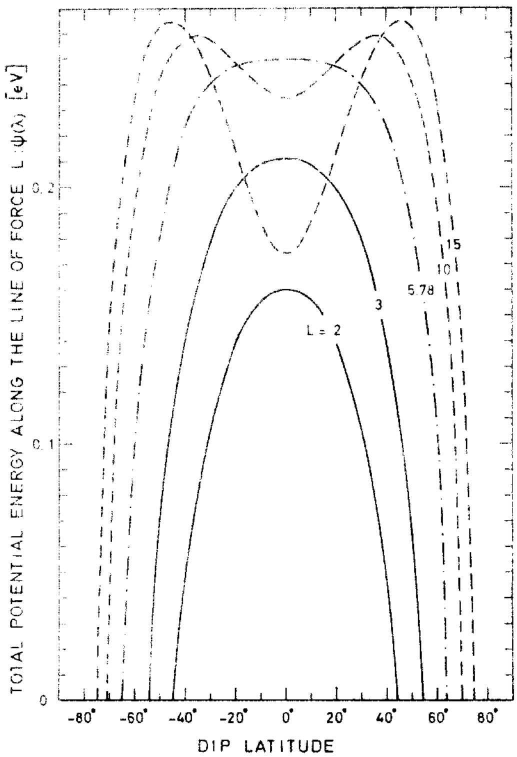

FIG. 2. GRAVITATIONAL PLUS ROTATIONAL POTENTIAL ENERGY OF AN H^+ ION OR AN ELECTRON ALONG DIFFERENT MAGNETIC FIELD LINES, COROTATING WITH THE EARTH.

For $L < 5{\cdot}78$ the total potential $\psi(\lambda)$ has one maximum at the Equator; for $L > 5{\cdot}78$, $\psi(\lambda)$ has a minimum at the Equator.

The critical L parameter (4) can be calculated for each local time angle, and the 'Roche-Limit' surface, $L = L_c$, can be deduced from the distribution of $\Omega(\mathbf{r})$. The solid line in Fig. 3 shows the equatorial section of the 'Roche-Limit' surface corresponding to McIlwain's quiet time electric and magnetic fields. Note that the smallest radial distance of the 'Roche-Limit' surface is $4{\cdot}5\ R_E$, near the midnight meridian.

3. DIFFUSIVE EQUILIBRIUM DENSITY DISTRIBUTIONS

If the collision time of the exospheric particles is smaller than the characteristic time for removing these particles from the inner magnetosphere by convection or precipitation, all types of orbits (ballistic and trapped) and all pitch angles will be equally populated. The velocity distribution will then be isotropic and a diffusive equilibrium model will result along the field line. Such steady state models have been described by Angerami and Thomas (1964), and reviewed by Bauer (1969).

The H^+ and electron density distribution along a field line L in an isothermal diffusion equilibrium model is given by the usual barometric formula

$$n(\lambda; L) = n_0 \exp\left[-\frac{\psi_{(\lambda)} - \psi_{(\lambda_0)}}{kT_0}\right] \tag{8}$$

where the potential distribution $\psi(\lambda)$ is given by Equation (3); n_0 is the density at the latitude λ_0 where the line of force L reaches the reference level h_0; T_0 is the kinetic temperature of the

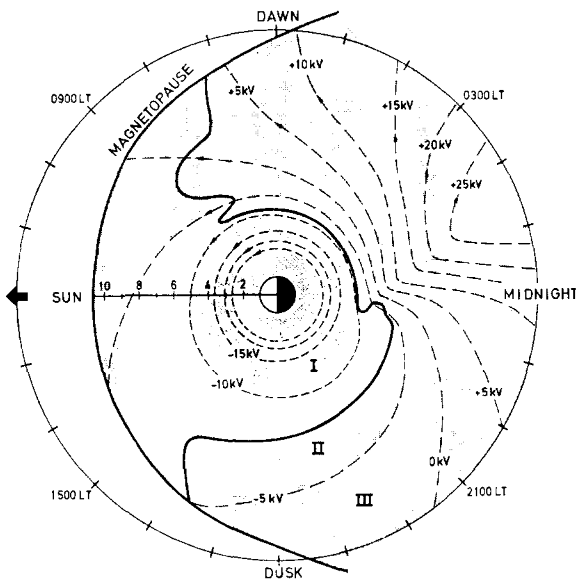

FIG 3. EQUATORIAL SECTION OF THE MAGNETOSPHERE.

The dashed curves are the equipotential lines for the electric field distribution E3 of McIlwain (1972). The solid line shows the 'Roche-Limit' $L = L_c$, for an angular drift velocity, $\Omega(r)$, determined by the radial component of the electric field E3. The plasmapause is the innermost equipotential surface tangent (near midnight) to the 'Roche-Limit' surface. The plasmaphere (shaded region I) is filled with nearly corotating thermal plasma held by the Earth's gravitational field. The shaded region III is the convection region of the magnetosphere, where any zero-energy particle will drift toward the magnetopause boundary and finally escape through the magnetotail. In the dayside portion of region II, the thermal particles have stable drift paths along the equipotential lines. Once this plasma has crossed the 'Roche-Limit' it is convected outwards in the night-time sector. The pressure gradient force will drive it across equipotential lines towards region III.

ionospheric electrons and protons. Along a field line with $L < L_c$, the density $n(\lambda;\ L)$ has a minimum at the Equator. But for $L > L_c$, the density distribution has a minimum at the points (r_m, $\pm\lambda_m$; Equations 5 and 6) where the gravitational plus centrifugal force has a zero component along the magnetic field direction. For $\lambda < \lambda_m$ and $r > r_m$ the density increases with altitude and it reaches a maximum at the equatorial plane.

The equatorial density distribution, $n(L)$ for $\Omega = \Omega_E$ is shown by the solid line D2 in Fig. 4. The dashed line D1 illustrates the equatorial density in a collision dominated model, when the rotational speed Ω is zero. The dot–dashed line D3 represents the equatorial density distribution when the angular rotational speed $\Omega(r)$ is evaluated along the 0200 LMT radial direction from the magnetic and electric field models M2 and E3 of McIlwain (1972). In all these three model calculations the H^+ ion and electron temperatures (1500°K) and densities ($2 \times 10^4\ cm^{-3}$) at the reference level (1000 km) are supposed to be independent of the dipole latitude λ_0.

It can be seen that the density at large distance increases when the angular velocity increases. For the non-rotating model D1, $n(L)$ decreases asymptotically to a constant value at $L = \infty$. When $\Omega = \Omega_E$ as in the corotating model D2, $n(L)$ has a minimum value at $L' = (\frac{2}{3})^{1/3}\ L_c = 6{\cdot}6$, and increases indefinitely beyond this radial distance. The D3 density distribution has a minimum at $L = 4{\cdot}5$. Below this radial distance $n(L)$ coincides

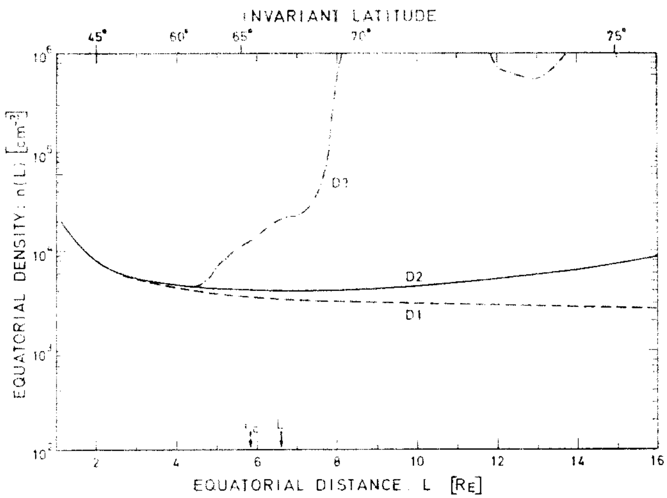

FIG. 4. EQUATORIAL DENSITY DISTRIBUTION CALCULATED FOR DIFFUSIVE EQUILIBRIUM, WITHOUT ROTATION (D1; $\Omega = O$), WITH UNIFORM ROTATION (D2; $\Omega = \Omega_E$), AND WITH NON-UNIFORM ROTATION (D3; $\Omega(\mathbf{r})$ DETERMINED ALONG THE 0200 LMT DIRECTION FROM MCILWAIN'S (1972) MAGNETIC AND ELECTRIC FIELDS DISTRIBUTION M2 AND E3).

In all these two-constituent models the ionospheric temperatures of electrons and H^+ ions are equal to 1500°K. The electron and H^+ ion densities at the reference level (1000 km) are also assumed to be independent of the dipole latitude λ_0: $n_0(H^+) = n_0(e^-) = 2 \times 10^4$ cm^{-3}.

approximately with the D2 distribution, since in this region McIlwain's E3 electric field is nearly equal to the corotational electric field, and, $\Omega(\mathbf{r}) \simeq \Omega_E$. However for $L > 4{\cdot}5$, McIlwain's electric field distribution predicts a large increase of $\Omega(\mathbf{r})$ with radial distance. The maximum density (7×10^6 cm^{-3}) is obtained at $L = 9$, where $\Omega(\mathbf{r})$ reaches a maximum value ($5{\cdot}43\ \Omega_E$) in the 0200 LMT meridian plane.

Beyond the Light-Ion-Trough (LIT) latitudes, oxygen ions gradually become the main ionic constituent at the altitude of 1000 km, and the electron and ion densities and temperatures depend on the latitude λ_0 (Thomas *et al.*, 1966, 1970; Brace *et al.*, 1967, 1970; Taylor *et al.*, 1965, 1968, 1972). Multi-constituent diffusive equilibrium models with variable reference level conditions are therefore required to describe the density profiles along field lines. Models of this type have been studied by Thomas and Angerami (1964), Thomas and Dufour (1965), Risbeth *et al.* (1966), Colin and Dufour (1968), Rycroft and Alexander (1969). The curve D4 in Fig. 5 gives the results obtained by Rycroft and Alexander (1969) for a corotating diffusive equilibrium plasmasphere model with latitude dependent reference level conditions reported by Sagredo and Bullough (1972). For comparison the curve D2 in Fig. 5 illustrates the equatorial density in a corotating diffusive equilibrium model with reference level conditions independent of the dipole latitude λ_0, as in the model D2 of Fig. 4. The positive density gradient obtained beyond $L = 4{\cdot}6$ in the corotating diffusive equilibrium model D4 with latitude dependent boundary conditions, is here a consequence of the increase of the relative O^+ ion concentration, the temperature, and the electron density for dipole latitudes larger than 58°. Therefore, the steep density gradient obtained beyond $L = 4{\cdot}5$ in model D3 where McIlwain's electric field distribution was used to calculate $\Omega(\mathbf{r})$, would be reinforced when realistic latitude dependent boundary conditions were used as in the model D4.

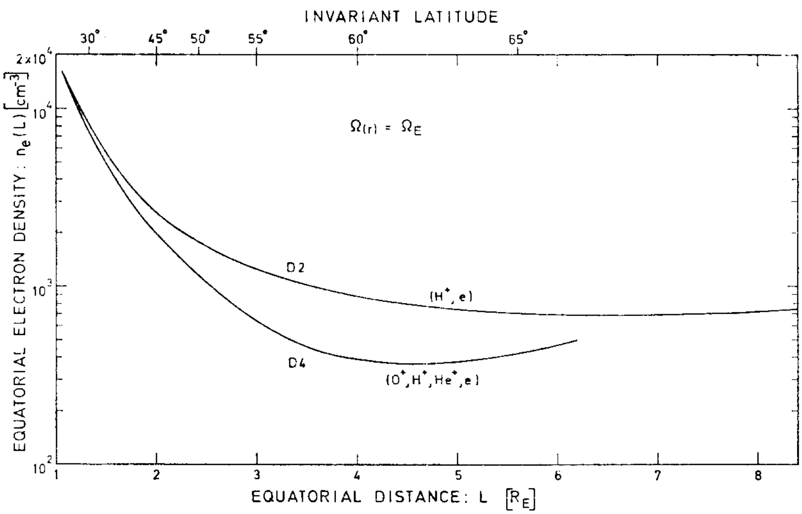

FIG. 5. EQUATORIAL ELECTRON DENSITY DISTRIBUTIONS FOR DIFFUSIVE EQUILIBRIUM WITH UNIFORM COROTATION ($\Omega = \Omega_E$).

The model D4 corresponds to a multi-component model with electron, H^+, O^+, He^+ ion temperatures and densities depending on the dipole latitude and taken from Sagredo and Bullough (1972). The model D2 corresponds to a two-constituent (H^+, e) model with reference level conditions at 900 km independent of the dipole latitude: $T_0 = 782°K$, $n_0(H^+) = n_0(e) = 1{\cdot}564 \times 10^4\ cm^{-3}$. These boundary values correspond to the equatorial temperature and electron density at 900 km in the model D4 of Rycroft and Alexander (1969).

4. THE PLASMAPAUSE BOUNDARY

From the results illustrated in Figs. 4 and 5, it can be deduced that, when $\Omega \neq 0$, positive density gradients in the radial direction (or along the magnetic field line) would exist for $L > L'$ (or $L > L_c$) in diffusive equilibrium models. Unless a sufficiently large kinetic pressure exists at large radial distance in the magnetosphere to maintain such positive density gradients, the diffusive equilibrium models D2 and D3 are convectively unstable beyond $L = L_c$. An outward expansion of the plasma will then occur spontaneously, trying to fill outer space and to build up there the required large pressure to make the static distributions D2 at D3 convectively stable. However the pressure gradient will force the particles located beyond the 'Roche-Limit' surface to penetrate into the outermost region III (in Fig. 3) where the convection motion will bring them on open magnetic field lines at the magnetopause boundary. (The inner edge of the shaded region III corresponds to the last closed field line limit for McIlwain's quiet time E3 model.) At the magnetopause these particles will finally escape into the magnetotail as suggested by Nishida (1966). Therefore the expected large thermal plasma pressure can never be build up in the region III of the outer magnetosphere, and consequently a continuous outward motion of trapped thermal particles originating from the trough ionosphere will result in the region beyond $L = L_c$. In the 'frozen-in' field concept (Gold, 1969; Sonnerup and Laird, 1963) this dynamical situation would be interpreted in terms of the interchange of magnetic field lines.

If the boundary of the shaded region I is defined as the innermost electric equipotential surface tangent to the 'Roche-Limit' surface (at $L = 4{\cdot}5$, near 2400 LMT for McIlwain's E3 model) no particle located inside this region will cross the 'Roche-Limit' surface during its corotation–convection diurnal motion. Since these particles will be stably trapped, it is suggested that the region I of Fig. 3 corresponds to the *plasmasphere* and its boundary to the quiet time ($K_p \simeq 1$) *plasmapause* position.

Any plasma evaporated from the ionosphere in the dayside portion of region II will at a certain time cross the 'Roche-Limit' surface, and will experience, in the nightside, an outward motion bringing it to region III. Therefore in region II corresponding to the midlatitude Light-Ion-Trough, a dynamical situation will result as in the polar wind: a given flux tube being gradually filled with ionospheric particles during the day and depleted of its thermal plasma content during the night. The upward field aligned particle fluxes suggested by the observations of Brinton *et al.* (1971) in the midlatitude topside ionosphere supports the conclusion that the exospheric plasma moves out of the region II into the region III where the density of the higher energy plasmasheet particles becomes predominant. The region II can be considered as a *plasmasheath* separating two different kind of plasmas: (1) the low temperature high density ionospheric plasma, and (2) the high temperature low density magnetospheric plasma. The *magnetosheath* is an other example of such a transition region between two different kind of plasmas: (1) the magnetosphere, and (2) solar wind plasmas.

Considering that the ballistic particles emerging from the dayside midlatitude ionosphere and put into trapped orbits by collisions are rapidly removed from the original flux tube by outward motion in the convectively unstable nightside portion of region II, it can be expected that, beyond $L = L_c$, the total density will mainly be due to the ballistic particle contribution as in the collisionless models of Eviatar *et al.* (1964) or Hartle (1969). Such exospheric models without trapped particles predict much smaller equatorial densities than diffusive equilibrium models; collisionless models are also in much better agreement with the observed r^{-4} density variation generally observed outside the plasmasphere (see Carpenter and Park, 1973; Chappell, 1972).

5. CONCLUSIONS

It is shown that the plasmapause formation is related to the existence of a 'Roche-Limit' surface where the components of the gravitational and centrifugal forces along the magnetic field direction balance each other. Even without any solar wind induced convection electric field, a plasmapause would exist and be located on a circle at $L = 5{\cdot}78$. In Fig. 3 we have shown how this 'Roche-Limit' surface is deformed by the quiet time convection electric field E3 of McIlwain (1972). This electric field distribution has been deduced from energetic (non-thermal) particle measurements at ATS 5 orbit. The plasmapause is identified with the innermost equipotential which is tangent to the 'Roche-Limit' surface (at $L = 4{\cdot}5$, near midnight where, according to Chappell *et al.* (1971), the level of magnetic activity determines the plasmapause position). The resulting shape and dimensions of the quiet time plasmasphere are in satisfactory agreement with the observations of Chappell *et al.* (1971) illustrated in Fig. 1.

In the present picture the plasmapause is not the last closed equipotential surface as in the earlier convection theories of the plasmapause formation. Indeed, in the unshaded region II of Fig. 3 the equipotential surfaces do not reach the magnetopause. The thermal plasma convecting in this region corresponding to the midlatitude LIT ionosphere, will necessarily cross the 'Roche-Limit' surface (solid line in Fig. 3) where the gravitational force is overtaken by the centrifugal force. The pressure gradient will force the particles to move outwards across the equipotential surfaces and ultimately bring them in the region III where they finally are lost at the magnetopause boundary, as suggested by Nishida (1966).

In region I corresponding to the plasmasphere the total ionization density is mainly constituted of thermal trapped particles, since the ballistic component gives a much smaller contribution at high altitudes. Diffusive equilibrium models are quite appropriate in this stable corotating region. Dynamical models with inter-hemispheric coupling, as studied by Mayr *et al.* (1972), are however necessary when the boundary conditions at magnetically conjugated points are not the same. In region III outside the last closed field line limit, collisionless models without trapped particles are more appropriate than diffusive equilibrium models which are unable to reproduce the observed densities. In the intermediate region II, local time varying models with uncomplete trapped particle population are more adequate to describe flux tube filling in the dayside and the outward convective motion in the nightside beyond the 'Roche-Limit' surface.

Acknowledgements—I would like to express my thanks to Prof. M. Nicolet for his support. I would like to express my appreciation to Drs. M. J. Rycroft and H. Volland for their valuable remarks and suggestions, as well as to Dr. M. Scherer for helpful discussions.

REFERENCES

ANGERAMI, J. J. and THOMAS, J. O. (1964). The distribution of electrons and ions in the earth's exosphere. *J. geophys. Res.* **69**, 4537–4560.
AXFORD, W. I. and HINES, C. O. (1961). A unifying theory of high-latitude geophysical phenomena and geomagnetic storms. *Can. J. Phys.* **39**, 1433–1464.
BAUER, S. J. (1969). Diffusive equilibrium in the topside ionosphere. *Proc. IEEE* **57**, 1114–1118.
BINSACK, J. H. (1967). Plasmapause observations with the MIT experiment on IMP 2. *J. geophys. Res.* **72**, 5231–5237.
BRACE, L. H., REDDY, B. M. and MAYR, H. G. (1967). Global behaviour of the ionosphere at 1000 km altitude. *J. geophys. Res.* **72**, 265–283.
BRACE, L. H, MAYR, H. G. and MAHAJAN, K. K. (1970). A polar maximum of electron concentration at 1000 km altitude. *J. atmos. terr. Phys.* **32**, 1945–1957.
BRICE, N. M., (1967). Bulk motion of the magnetosphere. *J. geophys. Res.* **72**, 5193–5211.
CARPENTER, D. L. (1966). Whistler studies of the plasmapause in the magnetosphere. I. Temporal variations in the position of the knee and some evidence on plasma motions near the knee. *J. geophys. Res.* **71**, 693–709.
CARPENTER, D. L. and PARK, C. G. (1973). On what ionospheric workers should know about the plasmapause-plasmasphere. *Rev. Geophys. Space Phys.* **11**, 133–154.
CHAPPELL, C. R. (1972). Recent satellite measurements of the morphology and dynamics of the plasmasphere. *Rev. Geophys. Space Phys.* **10**, 951–979.
CHAPPELL, C. R., HARRIS, K. K. and SHARP, G. W. (1971). The dayside of the plasmasphere. *J. geophys. Res.* **76**, 7632–7647.
CHEN, A. J. and WOLF, R. A. (1972). Effects on the plasmasphere of a time-varying convection electric field. *Planet. Space Sci.* **20**, 483–509.
COLIN, L. and DUFOUR, S. W. (1968). Charged particle temperature and concentrations in the Earth's exosphere. *J. geophys. Res.* **73**, 2967–2984.
DUNGEY, J. W. (1961). Interplanetary magnetic field and the auroral zones. *Phys. Rev. Lett.* **6**, 47–48.
EVIATAR, A., LENCHEK, A. M. and SINGER, S. F. (1964). Distribution of density in a ion-exosphere of a non-rotating planet. *Physics Fluids.* **7**, 1775–1779.
GOLD, T. (1959). Motions in the magnetosphere of the Earth. *J. geophys. Res.* **64**, 1219–1224.
GREBOWSKY, J. M. (1970). Model study of plasmapause motion. *J. geophys. Res.* **75**, 4329–4333.
GREBOWSKY, J. M. (1971). Time-dependent plasmapause motion. *J. geophys. Res.* **76**, 6193–6197.
HARTLE, R. E. (1969). Ion-exosphere with variable conditions at the baropause. *Physics Fluids* **12**, 455–462.
KAVANAGH, L. D., JR., FREEMAN, J. W. and CHEN, A. J. (1968). Plasma flow in the magnetosphere. *J. geophys. Res.* **73**, 5511–5519.
MANGE, P. (1960). The distribution of minor ions in electrostatic equilibrium in the high atmosphere. *J. geophys. Res.* **65**, 3833–3834.
MAYR, H. G., FONTHEIM, E. G. BRACE, H. L. BRINTON, H. C. and TAYLOR, H. A., JR. (1972). A theoretical model of the ionosphere dynamics with interhemispheric coupling. *J. atmos. terr. Phys.* **34**, 1659–1680.
MCILWAIN, C. E. (1972). Plasma convection in the vicinity of the geosynchronous orbit. *Earth's Magnetospheric Processes* (Ed. B. McCormac), pp. 268–279. Reidel, Dordrecht, Holland.

MELROSE, D. B. (1967). Rotational effects on the distribution of thermal plasma in the magnetosphere of Jupiter. *Planet. Space Sci.* **15**, 381–393.
NISHIDA, A. (1966). Formation of plasmapause, or magnetospheric plasma knee, by the combined action of magnetospheric convection and plasma escape from the tail. *J. geophys. Res.* **71**, 5669–5679.
RISHBETH, H., VAN ZANDT, T. E. and NORTON, R. B. (1966). Diffusive equilibrium in the topside equatorial ionosphere. *Annals. Géophys.* **22**, 538–548.
ROCHE, E., (1850). La figure d'équilibre d'une masse fluide soumise à l'attraction d'un point éloigné. *Mém. Acad. Montpellier.*
RYCROFT, M. J. and ALEXANDER, P. D. (1969). Model hydrogen and helium ion concentrations in the plasmasphere. Paper presented at 12th COSPAR Meeting, Prague.
RYCROFT, M. J. and THOMAS, J. O. (1970). The magnetospheric plasmapause and the electron density trough at the Alouette 1 orbit. *Planet. Space Sci.* **18**, 65–80.
SAGREDO, J. L. and BULLOUGH, K. (1972). The effect of the ring current on whistler propagation in the magnetosphere. *Planet. Space Sci.* **20**, 731–746.
SHAWHAN, S. D. and GURNETT, D. A. (1966). Fraction concentration of hydrogen ions in the ionosphere from VLF proton whistler measurements. *J. geophys. Res.* **71**, 47–59.
SONNERUP, B. U. O. and LAIRD, M. J. (1963). On magnetospheric interchange instability. *J. geophys. Res.* **68**, 131–139.
TAYLOR, H. A., JR., BRINTON, H. C. and SMITH, C. R. (1965). Positive ion composition in the magnetosphere obtained from the OGO A satellite. *J. geophys. Res.* **70**, 5769–5781.
TAYLOR, H. A. JR. and WALSH, W. J. (1972). The light-ion trough, the main trough and the plasmapause. *J. geophys. Res.* **77**, 6716–6723.
THOMAS, J. O. and DUFOUR, S. W. (1965). Electron density in the whistler medium. *Nature* **206**, 567–571.
THOMAS, J. O., RYCROFT, M. J. COLIN L. and CHAN, K. L. (1966). The topside ionosphere: II. Experimental results from Alouette I satellite. *Electron Density Profiles in Ionosphere and Exosphere* (Ed. J. Frihagen), pp. 322–357. North-Holland, Amsterdam.
THOMAS, J. O. and RYCROFT, M. J. (1970). The exospheric plasma during the International Years of Quiet Sun. *Planet. Space Sci.* **18**, 41–63.
VASYLIUNAS, V. M. (1970). Mathematical models of magnetospheric convection and its coupling to the ionosphere. *Particles and Fields in the Magnetosphere* (Ed. B. M. McCormac), pp. 60–71. Reidel, Dordrecht, Holland.
VASYLIUNAS, V. M. (1972). The interrelationship of magnetospheric processes. *Earth's Magnetospheric Processes* (Ed. B. M. McCormac), pp. 29–38. Reidel, Dordrecht, Holland.
VOLLAND, H. (1973). A semiempirical model of large-scale magnetospheric electric fields. *J. geophys. Res.* **78**, 171–180.
WOLF, R. A. (1970). Effects of ionospheric conductivity on convective flow of plasma in the magnetosphere. *J. geophys. Res.* **75**, 4677–4698.